



Systems Identification of a Cascade Controlled Servomechanism using Frequency Domain Analysis

B. E. Nyong-Bassey, A. M. Epemu*

Department of Electrical/Electronic Engineering, Federal University of Petroleum Resources Effurun, Nigeria.

*epemu.ayebatonye@fupre.edu.ng

Research Article

Abstract

In this paper experiments aimed at identifying the systems parameters of a cascade-controlled servomechanism using both the time domain step response method and frequency response domain Bode plot methods were investigated. In the cascade configuration, the velocity feedback attenuator gain caused the response to become overdamped. Hence, the overdamped response made the step response systems identification method inadequately as it requires at least an overshoot to correctly infer the systems transfer function. Nevertheless, using the frequency response based Bode plot it was possible to parameterise the transfer function of the servomechanism. Furthermore, the obtained model of the servomechanism, which was simulated in MATLAB, depicted the effect of varying the velocity feedback gain from 0.3 to 1 in both open and closed-loop configurations. Finally, the output response of the transfer function for the experimental servomechanism which was obtained via the frequency response method has been compared and validated against the experimental system's output response. Also, recent methods for systems identification of transfer function parameters based on genetic algorithm and particle swarm optimisation have been compared. The output of the transfer function model obtained via the frequency response-based method is in good agreement with the output response of the experimental servomechanisms. Hence, this validates the frequency response-based method.

Copyright © Faculty of Engineering, Ahmadu Bello University, Zaria, Nigeria.

Keywords

Feedback attenuator; Frequency Domain; Genetic algorithm; Servomechanism; Systems Identification;

Article History

Received: – November, 2021
Reviewed: – February, 2022

Accepted: – April, 2022
Published: – April, 2022

1. Introduction

Servomechanisms are at the core of modern robotics and mechatronics and more often, extensively used in industrial applications requiring extreme precision and speed performance indices (Miranda and Contreras, 2013). Nevertheless, controlling these servomechanisms to attain high-performance indices such as fast rise time and a small steady-state error, is not trivial and may require the application of model-based control systems techniques thus, necessitating the need for systems identification (Miranda and Contreras, 2013; M Hassan *et al.*, 2007; Lord and Hwang, 1977; Garrido and Miranda, 2006).

Systems identification involves mathematically deducing a model which describes the dynamics of a physical system or process using data obtained through a series of experimental measurements. Generically, systems identification is used for fault detection, parameter estimation, prediction, simulations and control design (M Hassan *et al.*, 2007).

Several systems identification techniques such as the step response time-domain method (Chen *et al.*, 2011; Kabita, 2015), Bode plot frequency response method (Samyгина *et al.*, 2019; Chen *et al.*, 2002), neural Fuzzy network (M Hassan *et al.*, 2007), nature-inspired optimisation techniques; particle swarm (Ding *et al.*, 2019), genetic algorithm (Pan *et al.*, 2021),

the grey wolf (Mohamed *et al.*, 2018; Mao and Hung, 2018) etc., have been proposed in literature.

In (Rake, 1979) a tutorial is presented with simple step response methods with periodic and non-periodic test signals to obtain models for dynamic processes. Furthermore, in (Okuyama *et al.*, 2015) frequency domain analysis with the bode diagram was used in a low-cost data acquisition setup to identify the parameters of an off-the-shelf DC motor, purchased without any information on the model parameters.

In (Chen *et al.*, 2002) a frequency response-based systems identification method using differential multifrequency binary test signals was proposed to simplify the behaviour of non-linear elements such as friction of a high-precision ball-screw table. In (Nayak and Shau, 2019) systems identification of a separately excited dc motor with unknown parameters was proposed to adopt a model via Whale optimisation to the reference armature current and speed obtained from experimental data. Similarly, in (Balamuruga and Mahalakshmi, 2017), the parameters of a BLDC controlled using Arduino were estimated using a Deep neural network (DNN) and BAT algorithm with the aid of reference speed, temperature, current and voltage of the BLDC motor.

Nevertheless, while state-of-the-art artificial intelligence-based systems identification methods such as neural network (NN) (Tutunji, 2016; Medsker and Bailey, 2020), genetic algorithm

(GA) (Piltan *et. al*, 2017), particle swarm optimisation (PSO) (Wu *et. al*, 2019); may suffice for the parameterisation of a grey or purely theoretical black-box model, these methods are computationally cumbersome, takes longer time to simulate and often without analytical insight.

Furthermore, the step response approach which is easy to use is undesirable for systems identification of higher-order transfer functions as it requires an underdamped response to infer the systems parameters, a limitation which the frequency response based Bode plot does not suffer. Hence, for the underscored reasons, the Bode plot frequency response-based technique will be adopted in the methodology.

In this paper, experiments will be performed on a cascade-controlled Servomechanism to obtain results using the Bode plot frequency response-based method to parameterise the servomechanism’s unknown transfer function. Furthermore, to determine the transfer function of the experimental servomechanism, the time domain step response, GA and PSO systems identification methods, are compared to the Bode plot approach. The comparison will be performed using both the transfer function model of the open and closed-loop servomechanism obtained using the Bode plot and simulated in MATLAB with the output responses compared in the time domain for easy visualisation and analysis.

Recent works of literature on systems identification of servomechanism have largely focused on artificial intelligence-based methods such as GA and PSO. However, these methods are inadequate for systems identification when the system exhibits underdamped oscillatory output responses especially in the case of cascade-controlled systems. Thus, this paper experimentally validates this key point with a focus highlighted on cascade-controlled systems.

However, the purpose of this paper is to emphasise the need to use bode plot frequency response-based systems identification method, in comparison with artificial intelligence methods such as GA and PSO. The transfer function model experimentally obtained Bode plot has not been compared to the GA and PSO methods.

2. Methodology

In this section, time-domain step response, and two pairs of frequency response-based experiments (that is Experiment 1 and 2, Experiment 3 and 4 are performed on the Servomechanism for the analysis with a sinusoidal input voltage of variable frequency. The first pair of the experiment for the frequency response technique involves the analysis of the Servomechanism with the speed feedback loop closed while the position feedback loop is open and the attenuator set at 0.3 and 1. Similarly, the second pair of experiments were performed with the attenuator set to 0.3 and 1 and the same input conditions as the former, however, both the speed and position closed-loop were connected to form a cascade configuration. Thereafter, a bode plot for each of the four (4) experiments, is obtained from which the frequency response parameters of the system can be determined and consequently the transfer function of the Servomechanism system.

2.1 Experimental Procedure Using Step Response Method

Experiment 0, the position control set up was done as shown in Figure 1. A square wave signal of amplitude (+/-5 volts) was applied as an input to the system and the velocity feedback signal was set to 0.2, 0.3, 0.4 and 0.6.

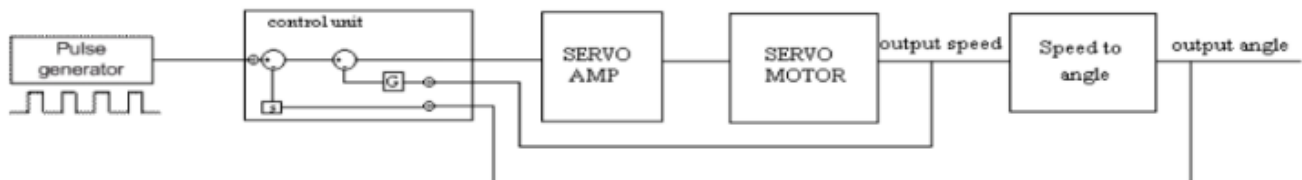


Figure 1: Closed-loop position control (Kabita, 2015)

The following are the measured steady-state error and maximum percentage overshoot for the attenuator gains, K as shown in Table 1.

Table 1: Steady-state error and corresponding overshoot in position control for attenuator values

Attenuator value	Steady-state error	Overshoot (%)
0.2	0.1	9.1
0.3	0.1	0
0.4	0.1	0
0.5	0.1	0

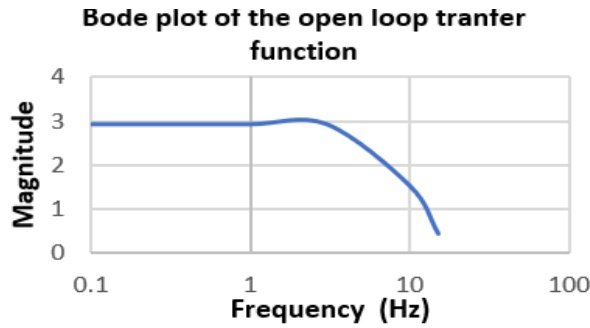
2.2 Experimental Procedure using Frequency Response

Experiment 1 was set up as shown in Figure 1, using an open feedback switch, a function generator that generated an input signal sine wave of magnitude 1 V and frequency of 0.1 Hz. The attenuator gain was set at 0.3 and the frequency varied

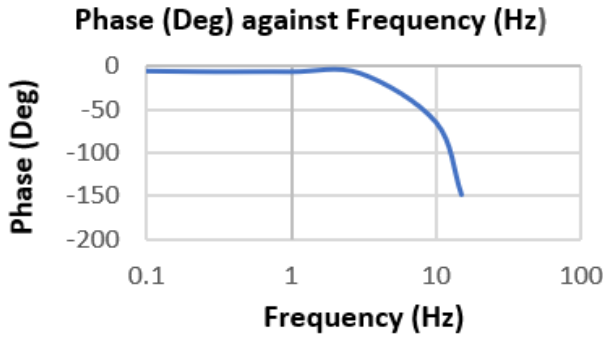
gradually as 0.1, 0.3, 1.0, 3.0, 10 and 15. Table 2 shows the speed controller output values, gain magnitude and phase shift values which were recorded using an oscilloscope trace. Figure 2 (a) and (b) shows the corresponding magnitude and phase bode plots obtained from Table 2.

Table 2: Gain values against frequency without position feedback loop with attenuator set at 0.3 and Input Voltage of 1.0V

Input Frequency (Hz)	Output Voltage (V)	Gain	Gain (dB)	Frequency (Rad/Sec)	Phase shift
0.1	3.5	2.916	9.297	0.628	-5.3
0.3	3.5	2.916	9.297	1.884	-6.1
1.0	3.5	2.916	9.297	6.283	-6.1
3.0	3.5	2.916	9.297	18.849	-8.0
10.0	1.8	1.500	3.521	62.831	-64.5
15.0	0.5	0.416	-7.618	94.247	-148



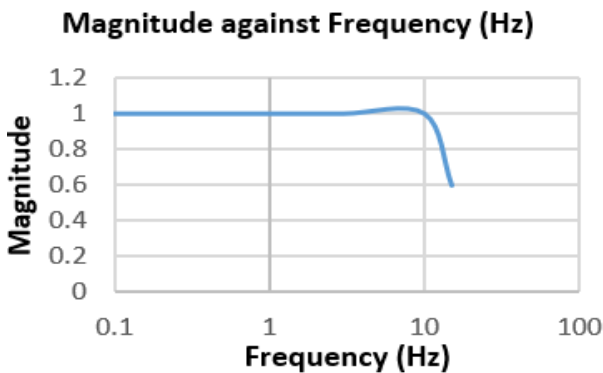
(a) Magnitude plot



(b) Phase plot

Figure 2: Bode Plot obtained from Experiment 1

Similarly, Experiment 2, was set up as presented in Experiment 1. However, the attenuator is set to 1. The results have been tabulated and shown in Table 3. And the Bode plot is shown in Figure 3.



Phase (Deg) against Frequency (Hz)

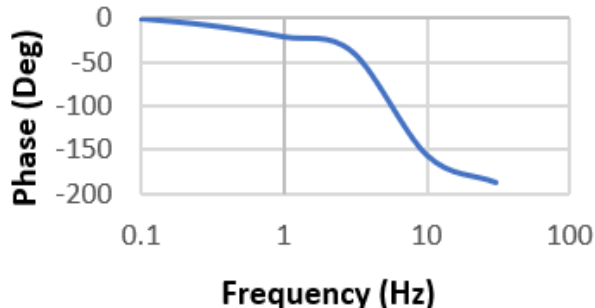


Figure 3: Bode Plot obtained from Experiment 2

Table 3: Gain values against frequency without position feedback loop with attenuator set at 1

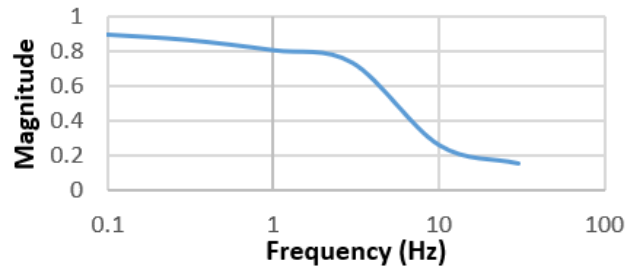
Input Voltage (V)	Frequency (Hz)	Output Voltage (V)	Gain	Gain (dB)	Frequency (Rad/Sec)	Phase shift
1.05	0.1	1.05	1.00	0.00	0.628	-0.3
1.05	0.3	1.05	1.00	0.00	1.884	-8.0
1.05	1.0	1.05	1.00	0.00	6.283	-21
1.05	3.0	1.05	1.00	0.00	18.849	-38
1.09	10.0	1.09	1.00	0.00	62.831	-156
1.09	15.0	0.60	0.60	-4.43	94.24	-186.5

In Experiment 3, a position feedback loop was connected, resulting in a cascade-controlled loop system with the attenuator set to 0.3 and a square wave reference input signal of magnitude 1 V was applied. The corresponding gain, frequency and phase shift for each input voltage were tabulated as seen in Table 4 with the Bode plot obtained from Table 4 as presented in Figure 4.

Table 4: Gain values against frequency for cascade control with attenuator set at 0.3

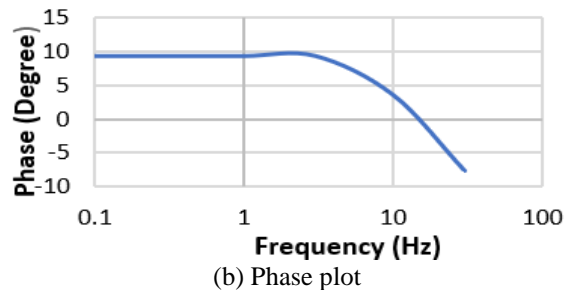
Input Voltage (V)	Output Voltage (V)	Frequency (Hz)	Gain	Gain (dB)	Frequency (Rad/Sec)	Phase shift
1.17	1.05	0.1	0.897	-0.944	0.628	-0.3
1.21	1.05	0.3	0.867	-1.239	1.884	-8.0
1.25	1.01	1.0	0.808	-1.851	6.283	-21
1.25	0.92	3.0	0.736	-2.662	18.849	-38
1.21	0.32	10.0	0.264	-11.56	62.831	-156
1.13	0.18	30.0	0.159	-15.97	188.495	-186.5

Magnitude versus frequency (Hz)



(a) Magnitude plot

phase (Deg) against Frequency (Hz)



(b) Phase plot

Figure 4: Bode Plot obtained from Experiment 3

Furthermore, Experiment 4 was set up as described in Experiment 3, however, the attenuator is set to 1. The results have been tabulated and shown in Table 5, with the Bode plot is shown in Figure 5.

Table 5: Gain values against frequency for cascade control with attenuator set at 1

Input Voltage (V)	Output Voltage (V)	Gain	Gain (dB)	Frequency (Hz)	Frequency (Rad/Sec)	Phase shift
3.06	3.06	1.00	0.00	0.1	0.628	-5.3
3.06	3.06	1.00	0.00	0.3	1.884	-5.3
3.06	2.25	0.74	-2.61	1.0	6.283	-43
3.06	1.17	0.38	-8.40	3.0	18.849	-66
3.10	0.28	0.09	-20.91	10.0	62.831	-134
3.06	0.14	0.05	-26.02	30.0	188.495	-178

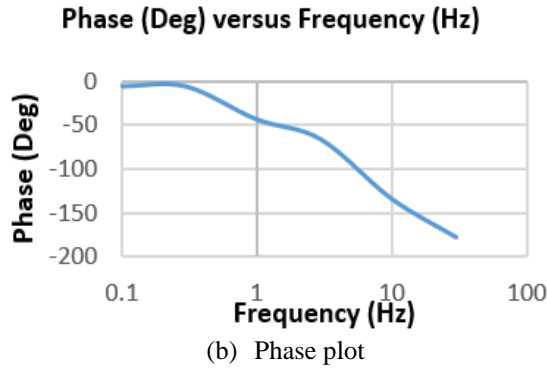
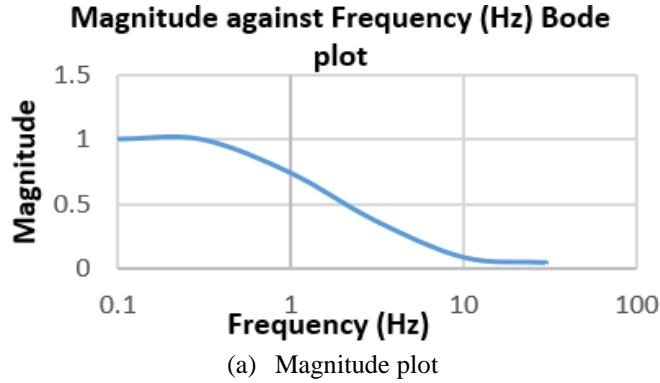


Figure 5: Bode Plot obtained from Experiment 4

2.3 Frequency response parameters estimation

From the Bode plot in Figure 2, the low-frequency gain K_{LF} is 2.916 and the break frequency w_c of 3Hz (18.84rad/s). The value of c is derived from the inverse of the low frequency gain (Kabita, 2015).

$$c = \frac{1}{K_{LF}} = \frac{1}{2.916} = 0.342 \quad (1)$$

d has been estimated using (2):

$$d = \frac{c}{w_c} = \frac{0.342}{(2 \times \pi \times 3)} = 0.0182 \frac{s}{rad} \quad (2)$$

The values of the natural frequency, w_n is obtained from (8):

$$w_n = \sqrt{\frac{6.65}{d}} = \sqrt{\frac{6.65}{(0.0182)}} = 19.115 \text{ rad/s} \quad (3)$$

Also, the value of ζ is estimated as

$$\zeta = \frac{w_n c}{2 \times 6.65} = \frac{(20.971 \times 0.285)}{2 \times 6.65} = 0.4915 \quad (4)$$

Since the system is underdamped, the frequency of the oscillation is given as in (5):

$$w_d = w_n \sqrt{(1 - \zeta^2)} = 19.115 \sqrt{(1 - 0.4915^2)} = 16.646 \text{ rad/s} \quad (5)$$

A summary of the frequency response parameters which were obtained from the experiments are presented in Table 6.

2.4 Transfer Function Estimation

The Speed closed-loop transfer function is obtained by substituting the parameters obtained from the Bode plot into the transfer function which is given by (6):

$$G(s) = \frac{1}{c + ds} \quad (6)$$

Thereafter, (6) is converted to open-loop position transfer function by multiplying $P(s)$ in (7):

$$T(s) = G(s)P(s) \quad (7)$$

Where, $P(s) = \frac{6.65}{s}$

Table 6: Summary of experimental frequency response parameters

Input Voltage (V)	Input Frequency (Hz)	Feedback attenuator gain	Low-Frequency gain (KLF)	Breakaway Frequency (w_c) in Hz	Natural Frequency (w_n) in rad/s	Damping ratio (ζ)	Damping frequency (w_d) in rad/s
1	0.1	0.3	2.916	3	19.115	0.4915	16.646
1	0.3	0.3	0.897	0.726	5.215	0.436	4.607
1	0.1	1	1	10	20.440	1.536	4.607
1	0.3	1	1	0.25	1.289	0.096	1.283

Therefore, in (8) the open-loop position transfer function for the servomechanism is:

$$T(s) = \frac{6.65}{(c + ds)s} \quad (8)$$

A simplified form of the transfer function in (8) is presented in (9) as follows:

$$T(s) = \frac{6.65/d}{c/ds + s^2} \quad (9)$$

Thus, equation (6) is then used to obtain the transfer function for the speed closed-loop servomechanism by substituting c and d as identified in Experiment 1:

$$G_{s1}(s) = \frac{54.94}{s + 18.79} \quad (10)$$

The open-loop Position transfer function is presented in (11):

$$\frac{\theta}{I} = G_{p1}(s) = \frac{54.94}{(s + 18.791)} * \frac{6.65}{s} = \frac{365.4}{s^2 + 18.795} \quad (11)$$

Consequently, the Speed closed-loop transfer function corresponding to the attenuator set at 1 as in Experiment 2, was deduced from the found parameters and presented in (12):

$$G_{s2}(s) = \frac{62.89}{s+62.89} \quad (12)$$

The open-loop position is also derived from the speed using (11):

$$\frac{\theta}{I} = G_{p2}(s) = \frac{62.89}{s+62.89} * \frac{6.65}{s} = \frac{418.21}{62.89s+s^2} \quad (13)$$

Therefore, the close loop transfer function is obtained by substituting the frequency response parameters obtained from the Bode plot into the close loop transfer function in (14) which is given by:

$$\frac{\theta}{I} = \frac{6.65/d}{s^2 + \frac{c}{d}s + \frac{6.65}{d}} \quad (14)$$

Therefore, the transfer function for the close loop position servomechanism when attenuator was set to 0.3 in Experiment 3, is presented in (15):

$$G_{p3}(s) = \frac{27.25}{s^2+4.56s+27.25} \quad (15)$$

While the closed-loop position transfer function when attenuator was 1 in Experiment 4, is presented in (16):

$$G_{p4}(s) = \frac{1.66}{s^2+0.25s+1.66} \quad (16)$$

3. Experimental Results and Discussion

This section analyses and discusses the results obtained from the step response method in Experiment 0 and the frequency response-based Experiments 1 to 4 for systems identification of the Servomechanism parameters.

3.1 Step Response Approach

In Experiment 0, the velocity feedback loop is used to damp out the oscillation as its gain is increased thereby eliminating the overshoot, this is like a derivative action. However, the steady-state error persists due to the absence of integral action.

3.2 Bode Plot Frequency Response Approach

In Experiment 1, the Bode plot in Figure 2, has been used to determine the natural frequency ω_n , the low-frequency gain K_{LF} and damping ratio ζ which was further used to derive the system transfer function parameters as shown in the result section. The damping ratio was found to be 0.4915 which is acceptable (that is less than 1).

In Experiment 2, the Servomechanism behaves linearly because, from the step response, it is an underdamped response typical of a second-order close loop system. Also, the response corresponds to the calculated value of damping ratio ζ which was 0.436, as this shows the system response will exhibit overshoot with a natural frequency of 5.215 rad/s. However, the damping ratio is within the desired range of value (that is less than 1).

In Experiment 3, the calculated value of damping ratio ζ is 1.536, which is above the desired range (that is less than 1) as such, the Servomechanism's response in the time domain is overdamped. Hence, the system behaves sluggishly with no overshoot and the transfer function parameters will be difficult to determine using the step response method.

In Experiment 4, the servomechanism behaves linearly because from the step response it is an underdamped response typical of a second-order close loop system. Also, the time domain response corresponds to the calculated value of damping ratio ζ which was 0.096 as this shows the system response will exhibit undesired overshoot with a natural frequency of 1.289 rad/s.

3.3 Simulation Model Validation of Servomechanism

The servomechanism transfer functions have been determined as $G(s)$, therefore the output response of the servomechanism can be simulated from the derived transfer functions.

the servomechanism closed-loop step responses for speed and position were determined from the parameters obtained in Experiments 1 to 4, from the Bode plot. Therefore, the two-speed closed loop and the two-position closed-loop responses from Experiments 1 and 2, and Experiments 3 and 4 respectively, have also been compared in this section.

3.3.1 Velocity Feedback Without a Position Feedback Loop

The closed-loop speed step response has been compared and from the investigation, the effect of increasing the attenuator from 0.3 to 1 reduces the steady-state value and reduces the rise time as shown in Table 7. This indicates that the open-loop is sensitive to the attenuator gain and will not attain the desired output response when the loop gain changes. However, an advantage is that there is no overshoot as the response is always overdamped, typical of a first-order system.

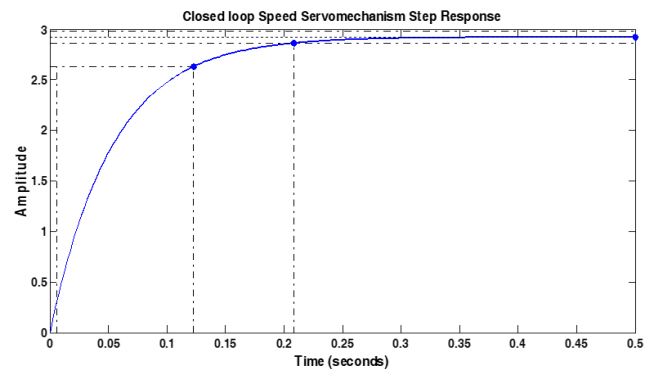


Figure 6: Closed-loop Speed Servo response when the attenuator was set at 0.3.

Table 7: Transient response characteristics for the speed closed-loop servo response

	Attenuation 0.3	Attenuation 1
Settling time	0.208 seconds	0.0622 seconds
Rise time	0.117 Seconds	0.0349 seconds
Steady-state value	2.92	1

Table 7 compared the two closed-loop speed transient responses of the servo when the attenuator is 0.3 and 1.

For the closed-loop speed control Figure, 6 and 7 shows the response when the attenuator was 0.3 and 1, respectively.

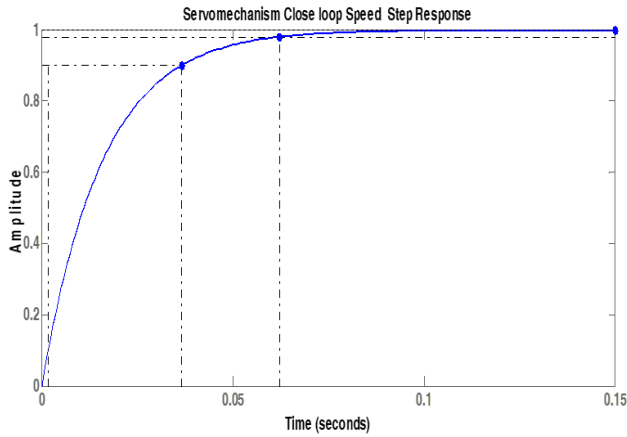


Figure 7: Closed-loop Speed Servo response when the attenuator was set at 1.

3.3.2 Velocity Feedback with Position Feedback loop (Cascade Control)

Also comparing the two closed-loop position responses using the Bode plot approach, shown in Figures 8 and 9 when attenuator was 0.3 and 1 with closed position feedback switch. The closed-loop position step responses show an increase in percent overshoot which is beyond the acceptable range as the attenuator gain is changed 0.3 to 1. Similarly, the effect of increasing the attenuator gain from 0.3 to 1 increases the settling time and increases the rise time. The oscillatory response becomes increasingly undesirable with an increase in the attenuator gain from 0.3 to 1 as the velocity feedback damping effect results in an underdamped response. The oscillation underscores the disadvantage of using the closed-loop control system despite the benefit of tracking the reference input. Table 8 compares the two closed-loop position transient responses of the servo when the attenuator is 0.3 and 1 using the Bode plot method.

To investigate GA and PSO, a fitness function based on the integral squared error was used. The GA and PSO were used to curve fit and estimate transfer function parameters that match the output response obtained via experiment and analysis of the servomechanism using the frequency response method. Since the servomechanism was not explicitly known ab initio, in estimating the parameters which populate the transfer function parameters of the DC servomechanism, a feasible range of values to be optimised were obtained from literature (Fox, 2005; Nyong-Bassey and Akinloye, 2014). The output response of the transfer function obtained using the GA and PSO methods were validated against the experimentally obtained output response of the servomechanism. Furthermore, when the attenuator was 0.3, the corresponding closed-loop position responses with GA and PSO methods were used to identify the transfer function structure of the servomechanism. Figures 10 and 11 shows the GA and PSO output response, while Figure 12 shows the

experimental output plot of the servomechanism closed-loop position response for attenuator set at 0.3.

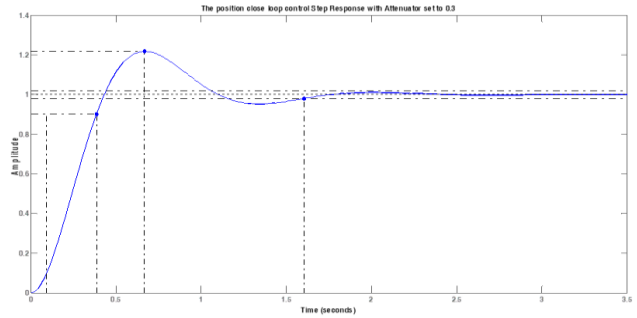


Figure 8: Position closed-loop servo response when the attenuator was set at 0.3

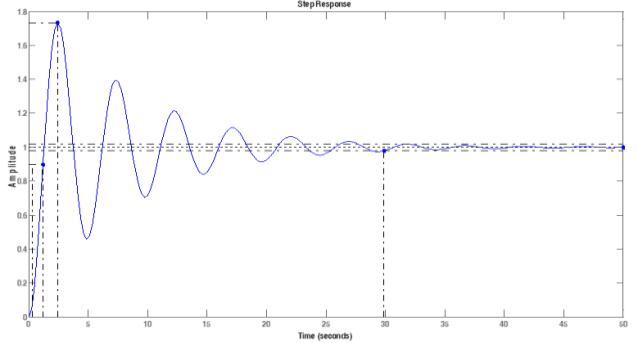


Figure 9: Bode method Position closed-loop servo response when the attenuator was set at 1

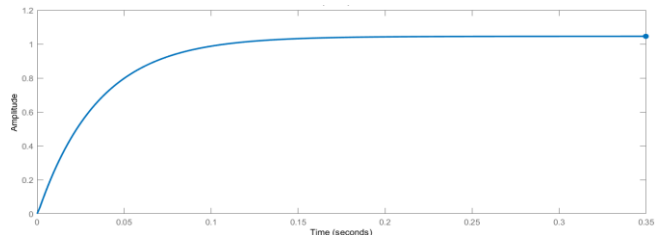


Figure 10: GA closed-loop response with Attenuator at 0.3

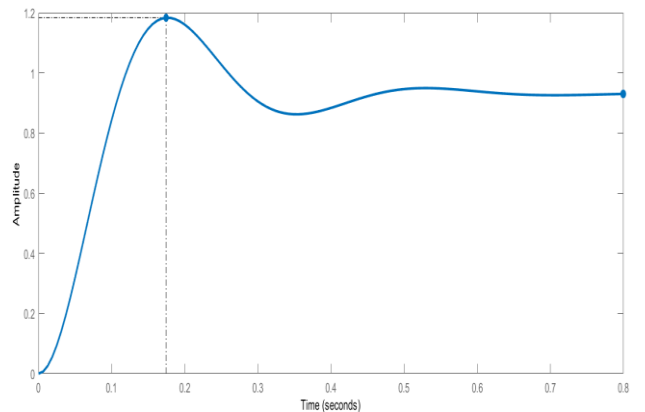


Figure 11: PSO closed-loop response with Attenuator at 0.3

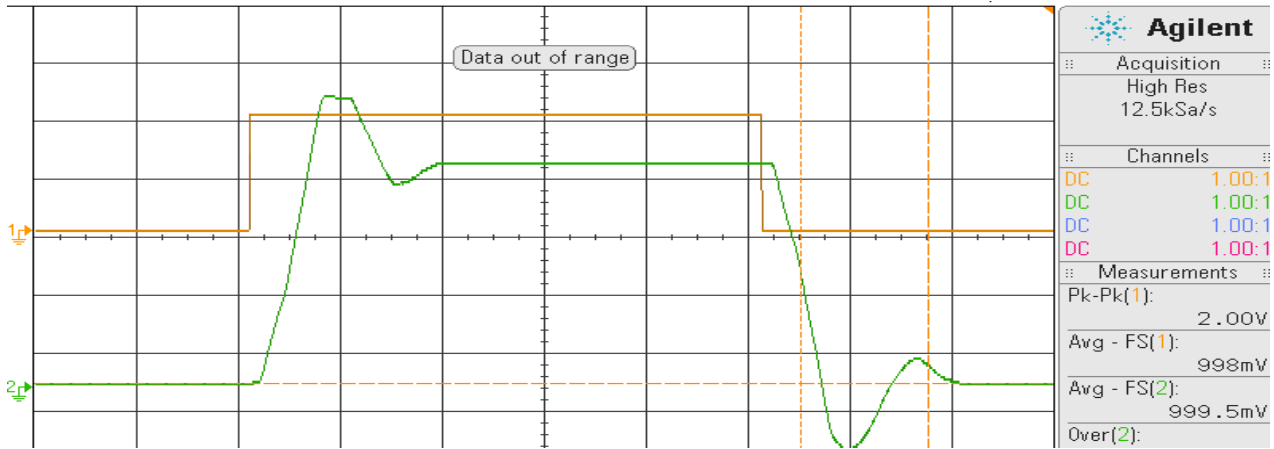


Figure 12: DC Servomechanism closed-loop position response with attenuator set to 0.3 obtained experimentally

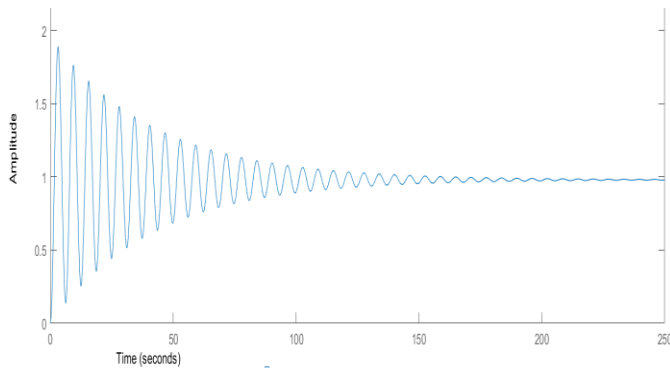


Figure 13: GA closed-loop position response with attenuator set at 1

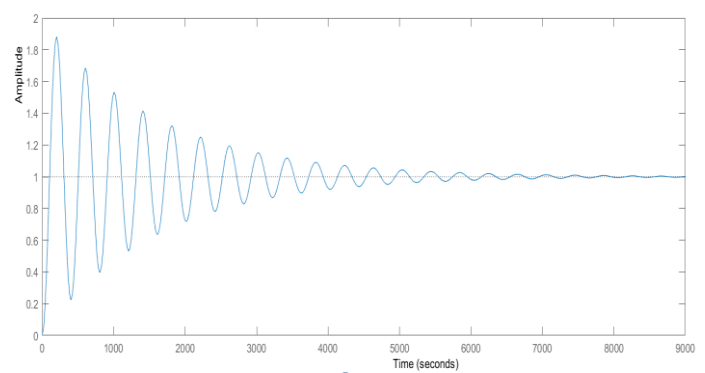


Figure 14: PSO closed-loop position response with attenuator set at 1

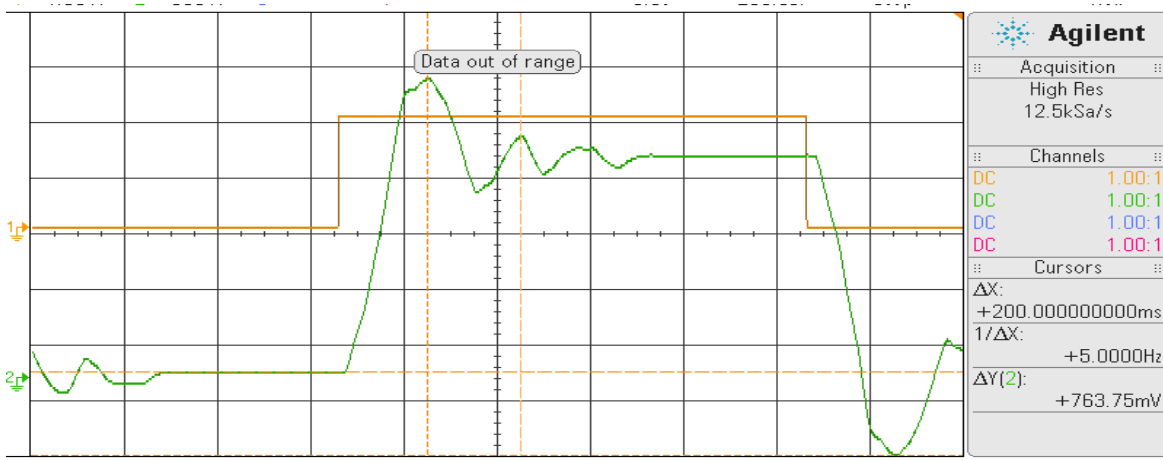


Figure 15: DC Servomechanism closed-loop position response with attenuator set to 1 obtained experimentally via an oscilloscope

Table 8: Comparison of Transient response characteristics for the position closed-loop response between Bode, GA and PSO methods against Experimental Servomechanism with attenuator set at 0.3

	Experimental	Bode plot	GA	PSO
Settling time (sec)	1.5	1.6	0.15	0.61
Steady-state value	1	1	1.04	0.92
Rise time (Sec)	0.2	0.292	0.1	0.1
% Overshoot (%)	25.2	21.8	0	12

Simulation runtime (sec)	Real-time	2.41	150	26.29
Fitness score	-	-	0.5179	0.04

Similarly, Figures 13 and 14 show the GA and PSO output response alongside Figure 15 which shows the experimental output of the servo mechanism when the attenuator was set at 1.

Table 9: Comparison of Transient response characteristics for the position closed-loop response between Bode, GA and PSO methods against Experimental Servomechanism with attenuator set at 1

	Experimental	Bode plo	GA	PSO
Settling time (sec)	1.2	29.9	200	7000
Steady-state value	1	1	1	1
Rise time (sec)	0.2	0.872	1.6	100
Percentage Overshoot (%)	39.2	73.6	81	82
Simulation runtime (sec)	Real-time	2.48	160	26.5
Fitness score	-	-	0.044	0.043

4. Conclusion

This paper carried out an experimental investigation for system identification and parameter estimation of a cascade-controlled servomechanism using the Bode plot frequency response-based technique. The DC gain of the servomechanism was determined for a range of input voltages, ± 5 V.

In the analysis, it was observed that the input voltage was inversely proportional to the DC gain of the Servomechanism. As the input voltage was increased the DC gain of the Servomotor decreased while the time constant remained constant to both forward and reverse rotation was determined. To analyse the time domain response of the servomechanism as well as identify the servo system parameters, the step response approach was investigated in open and closed-loop configurations, where only the velocity feedback loop was connected without the position feedback loops and as well as in cascade. However, in the analysis, the step response method had a drawback as it required at least one overshoot for system parameters determination in the close loop response. Therefore, in the cascaded control configuration, the introduction of the velocity feedback loop introduced in the position closed-loop control made the step response method inadequate. The inadequacy of the step response method was because the velocity feedback damped out the oscillation which is required when using the step response method. This contrasts with the Bode plot which is a frequency response-based method that does not depend on a minimum overshoot like the step response. Hence, the Bode plot approach which is frequency response based and independent of system order is a better method for system identification than the step response method.

Furthermore, from the experiment, the inclusion of a velocity feedback loop to make a closed-loop position control system stable does not always yield a desirable response. As observed when the attenuator was increased the underdamped second-order response became increasingly oscillatory due to the velocity feedback loop. While in the close-loop speed control as the attenuator was increased the system became faster however with a reduction in the open-loop gain.

The efficacy of artificial intelligence-based systems identification methods such as GA and PSO diminishes as the damping ratio of a system decreases such as when the attenuator was increased from 0.3 to 1. As seen in Tables 8 and 9, despite a low fitness function performance index, the output response was not an exact or close match when the attenuator was set at 1. The PSO which is a faster algorithm than GA had a better transient response than GA when the attenuator was 0.3. However, the GA gave a better response than the PSO when the attenuator was increased to 1.

Thus, the frequency response-based systems identification is preferred since it gave the most optimum results and was a better match, transient characteristics in contrast to the rest methods irrespective of the response type or characteristics as shown in Table 8 and 9.

References

- Balamuruga, K., & Mahalakshmi, R. (2017). Parameter Identification in BLDC Motor using Optimization Technique. *Journal of Applied Science and Engineering Methodologies*, 3(2), 465-470.
- Chen, L., Li, J., & Ding, R. (2011). Identification for the second-order systems based on the step response. *Mathematical and computer modelling*, 53(5-6), 1074-1083.
- Chen, Y. Y., Huang, P. Y., & Yen, J. Y. (2002). Frequency-domain identification algorithms for servo systems with friction. *IEEE transactions on control systems technology*, 10(5), 654-665.
- Ding, J., Wang, Q., Zhang, Q., Ye, Q., & Ma, Y. (2019). A hybrid particle swarm optimization-cuckoo search algorithm and its engineering applications. *Mathematical Problems in Engineering*, 2019.
- Fox, H. (2005). An interdisciplinary control systems course for engineering technologists: Description of lecture topics and laboratory experiments. *In 2005 Annual Conference* (pp. 10-190).
- Garrido, R., & Miranda, R. (2006, October). Closed-loop identification of a DC servomechanism. *In 2006 IEEE International Power Electronics Congress* (pp. 1-5). IEEE.
- Kabita A. (2015), EEE 8074 Servomechanism and Systems Identification Laboratory Notes, Newcastle University.
- Lord, W., & Hwang, J. H. (1977). DC servomotors-modelling and parameter determination. *IEEE Transactions on Industry Applications*, (3), 234-243.
- Mao, W. L., & Hung, C. W. (2018). Type-2 fuzzy neural network using grey wolf optimizer learning algorithm for nonlinear system identification. *Microsystem Technologies*, 24(10), 4075-4088.
- M Hassan, M., A. Aly, A., & F Rashwan, A. (2007). Different Identification Methods with Application to a DC Motor. *JES. Journal of Engineering Sciences*, 35(6), 1481-1493.
- Medsker, L. R., and Bailey, D. L. (2020). Models and guidelines for integrating expert systems and neural networks. *In Hybrid architectures for intelligent systems* (pp. 153-171). CRC Press.

- Miranda Colorado, R., & Contreras Castro, G. (2013). Closed-loop identification applied to a DC servomechanism: controller gains analysis. *Mathematical Problems in Engineering*, 2013.
- Mohamed, O. A., Okasha, A., & Abdrabbo, S. (2018). Online Identification and Artificial Intelligence Control of a Servo Pneumatic System. *Scientific Journal of October 6 University*, 4(2), 60-65.
- Nayak, B., & Sahu, S. (2019). Parameter estimation of DC motor through whale optimization algorithm. *International Journal of Power Electronics and Drive Systems*, 10(1), 83.
- Okuyama, I. F., Maximo, M. R. O. A., & Pinto, S. C. (2015). System identification of a hobby dc motor using a low-cost acquisition setup. *Simpósio Brasileiro de Automação Inteligente (SBAI)*.
- Nyong-Bassey, B. E., and Akinloye, B. (2014). Comparative study of optimised artificial intelligence-based first order sliding mode controllers for position control of a DC motor actuator. *Journal of Automation, Mobile Robotics and Intelligent Systems*, 58-71.
- Pan, Y., Liu, X., Zhu, Y., Liu, B., & Li, Z. (2021). Feedforward Decoupling Control of Interior Permanent Magnet Synchronous Motor with Genetic Algorithm Parameter Identification. *Progress In Electromagnetics Research M*, 102, 117-126.
- Piltan, F., TayebiHaghighi, S., and Sulaiman, N. B. (2017). Comparative study between ARX and ARMAX system identification. *International Journal of Intelligent Systems and Applications (IJISA)*, 9(2), 25-34.
- Rake, H. (1979). Step response and frequency response methods. *IFAC Proceedings Volumes*, 12(8), 519-526.
- Samygina, E., Tiapkin, M., Rassudov, L., & Balkovoi, A. (2019). Extended Algorithm of Electrical Parameters Identification via Frequency Response Analysis. In *2019 26th International Workshop on Electric Drives: Improvement in Efficiency of Electric Drives (IWED)* pp. 1-4.
- Tutunji, T. A. (2016). Parametric system identification using neural networks. *Applied Soft Computing*, 47, 251-261.
- Wu, Z., Yang, R., Guo, C., Ge, S., & Chen, X. (2019). Analysis and Verification of Finite-Time Servo System Control with PSO Identification for Electric Servo System. *Energies*, 12(18), 3578.